ORGANIC MASS SPECTROMETRY, VOL. 22, 259-268 (1987)

OH$^{\cdot}$ Loss and Molecular Rearrangements of Quinoxaline *N*-Oxides Studied by Interpretation of Mass Spectra and Application of Linear Discriminant Analysis

M. Bartoszek, D. Salzwedel, G. Stumm and H.-J. Niclas
Akademie der Wissenschaften der DDR, Zentralinstitut für Organische Chemie, Rudower Chaussee 5, DDR-1199 Berlin, GDR

Quinoxaline *N*-oxides substituted at the *ortho* position to the NO group give characteristic $[M-OH]^+$ fragments. With the di-*N*-oxides the peak intensities depend on the electron-withdrawing strength of the 2- and 3-substituents. Linear discriminant analysis was used to study the fragmentation of quinoxaline *N*-oxides as determined by the number of NO groups. Results of peak selection and discriminant analysis (Fisher quotients and discriminant vector coefficients) were interpreted with regard to the mass spectrometric decomposition of quinoxaline and quinoxaline *N*-oxide molecules. For the substituted quinoxaline *N*-oxides, fragmentations involving molecular rearrangements like those observed for unsubstituted quinoxaline *N*-oxides were also found. For these compounds, partial rearrangement to quinoxalinones is confirmed.

Owing to their activity as growth promotants,[1] quinoxaline di-*N*-oxides have of late attracted considerable attention and interest. Their reduction products are important metabolites.[2,3] For this reason, studies of mass spectrometric fragmentation processes of quinoxalines and quinoxaline mono- and di-*N*-oxides were carried out. The influence of substituents at the C(2) and C(3) atoms on electron impact (EI) induced loss of oxygen and the influence of the number and position of NO groups on the degradation of the quinoxaline molecule are discussed in detail. A list of compounds studied is presented in Table 1.

N-Oxides of pyridines, benzimidazoles and a number of quinoxalines have already been the subject of several studies.[4-9] These studies were, however, confined to the investigation of correlation between the nature and position of substituents and the loss of oxygen in *N*-oxides. In the compounds with an alkyl substituent in the *ortho* position to the NO group, it was found that oxygen is abstracted as an OH$^{\cdot}$ radical. Thus, for 2-alkylquinoxaline 1-oxides investigated by Tatematsu *et al.*[4] the peak ratio $[M-OH]/[M]$ has values $Q_m > 1$. For the quinoxaline di-*N*-oxides they postulate a primary elimination of an oxygen atom, giving $Q_f < 1$ with $Q_f = [M-OH]/[M-O]$. For 2-alkylpyridine *N*-oxides, Lightner *et al.*[5] reported metastable peaks indicating OH$^{\cdot}$ radical loss, but for 3- and 4-alkylpyridines, with a significant lower intensity of the corresponding peaks, a two-step reaction gives $[M-O-H]^+$ ions. They also showed that changes in local electron density upon oxidation of pyridines result in abundant $[M-15]^+$ fragments with 4-ethylpyridine *N*-oxide, whereas with non-oxidized ethylpyridines the corresponding fragment appears with the 3-ethylpyridine.

RESULTS AND DISCUSSION

Loss of oxygen

All the quinoxaline *N*-oxide spectra in this study show $[M-17]$ peaks, corresponding to the loss of an OH$^{\cdot}$ radical from the molecular ion (Table 1). These peaks mostly appear with high intensity. The *ortho* effect leads to Q_m values greater than 1 with compounds **11** and **18**. The situation with the compounds **14-17** is more difficult. The 15 eV spectra of **16** and **17** show extremely different $[M-OH]$ peak intensities (Fig. 1). Introduction of an *N*-(2-hydroxyethyl)carbamoyl group in the *ortho* position to the NO group leads to a forced loss of an OH$^{\cdot}$ radical. This indicates the *ortho* effect to be dominated by the carbamoyl substituent. $[M-OH]^+$, m/z 230, and the subsequent loss of R^2 leading to the methylquinoxaline fragment m/z 143 give the most intense peaks in the spectrum of **17**. In contrast, the abundant molecular ion and $[M-18]^{+\cdot}$, $[M-31]^+$ and $[M-R^2]^+$ fragments (m/z 247, 229, 216 and 159) with compound **16** indicate that the loss of OH$^{\cdot}$ is less favoured with a methyl group in the *ortho* position to the oxygen. In this case the molecular ion is more stable and competing reactions lead to the more intense peaks relative to $[M-OH]^+$.

Interesting results are given by di-*N*-oxides. The $[M-OH]^+$ fragment appears as the sum of competing products because both the substituents are in the *ortho* position. Inspection of the Q_m values shows that the variance

0030-493X/87/050259-10$05.00

Received 23 July 1986
Accepted 3 November 1986

Table 1. Compounds studied and quinoxaline *N*-oxide mass spectral data characteristic of the loss of oxygen

Compound	R^1	R^2	Oxide	*M*	Q_m	Q_f	References
1	CH_3	H	—	21.9	—	—	19
2	COOH	CH_3	—	5.4	—	—	20
3	$COOCH_3$	CH_3	—	15.2	—	—	11
4	$COOC_2H_5$	CH_3	—	2.0	—	—	21
5	$CONHC_2H_4OH$	CH_3	—	0.8	—	—	[a]
6	$CH{=}NC_6H_5$	H	—	12.5	—	—	22
7	$CH{=}NC_6H_4CH_3(p)$	H	—	9.5	—	—	23
8	$CH{=}NC_6H_4Cl(p)$	H	—	7.6	—	—	24
9	$CH{=}NC_6H_4NO_2(p)$	H	—	1.5	—	—	[a]
10	$CH{=}NC_6H_4NO_2(m)$	H	—	1.3	—	—	[a]
11	CH_3	H	1	19.8	1.1	36.3	19
12	CH_3	COOH	1	4.3	0.8	6.5	11
13	$COOCH_3$	CH_3	1	13.5	0.3	2.8	11
14	$COOC_2H_5$	CH_3	1	5.2	0.1	8.9	25,[a]
15	CH_3	$COOC_2H_5$	1	15.4	0.1	1.9	[a]
16	$CONHC_2H_4OH$	CH_3	1	0.4	19.1	11.1	[a]
17	CH_3	$CONHC_2H_4OH$	1	7.5	0.5	11.7	[a]
18	$-CH_2-CH_2-CH_2-CH_2-$		1	3.9	2.5	21.5	26
19	H	H	1, 4	27.3	0.1	0.3	19
20	CH_3	H	1, 4	13.0	0.2	2.8	19
21	C_2H_5	H	1, 4	13.3	1.0	11.9	19
22	CH_2OH	H	1, 4	0.5	3.5	3.7	19
23	CH_2Br	H	1, 4	2.6	0.7	7.2	19
24	CH_3	CH_3	1, 4	10.9	0.3	8.5	19
25	CHO	CH_3	1, 4	5.1	2.3	20.5	19
26	COOH	CH_3	1, 4	0.1	0.7	0.8	19
27	$COOCH_3$	CH_3	1, 4	16.6	0.4	6.7	19
28	$COOC_2H_5$	CH_3	1, 4	3.5	0.1	0.8	19
29	$COOC_2H_4OH$	CH_3	1, 4	3.4	0.1	0.1	27
30	$CONH_2$	CH_3	1, 4	3.6	2.2	12.7	28
31	$CONHCH_3$	CH_3	1, 4	1.7	4.0	12.7	28
32	$CON(CH_3)_2$	CH_3	1, 4	0.6	9.0	45.8	28
33	$CONHC_4H_9(n)$	CH_3	1, 4	0.9	7.8	26.1	29
34	$CONHC_2H_4OH$	CH_3	1, 4	2.7	4.6	20.1	29
35	$CON(C_2H_4OH)_2$	CH_3	1, 4	0.3	4.0	14.7	[a]
36	$CONHC_2H_4OH$	CH_2Br	1, 4	0.5	4.6	35.7	[a]
37	$CONHC_2H_4OH$	CH_2OCOCH_3	1, 4	0.2	1.8	23.7	[a]
38	$CH{=}NC_4H_9(n)$	H	1, 4	0.6	2.3	15.3	[a]
39	$CH{=}NC_6H_{11}$(cyclo)	H	1, 4	1.0	2.5	25.6	[a]
40	$CH{=}NC_6H_5$	H	1, 4	0.8	14.0	13.5	30,[a]
41	$CH{=}NC_6H_4CH_3(p)$	H	1, 4	0.7	17.2	30.9	30,[a]
42	$CH{=}NC_6H_4Cl(p)$	H	1, 4	0.2	17.8	23.1	30,[a]
43	$CH{=}NC_6H_4NO_2(m)$	H	1, 4	0.6	10.7	15.6	30,[a]
44	$-CH_2-CH_2-CH_2-CH_2-$		1, 4	9.2	0.6	15.6	28

M = intensity of the molecular ion peak in % Σ_{45}.
$Q_m = [M-OH]/[M]$.
$Q_f = [M-OH]/[M-O]$.
[a] See Experimental section.

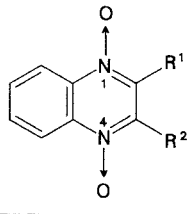

within the substituent groups is smaller than between the groups. The Q_m value ranges (Table 2) suggest a relationship between $OH^\cdot$ loss and the electron-withdrawing strength of the *ortho* substituent. The effect of electron-withdrawing groups on the reduction of quinoxaline *N*-oxides is known from the reaction with trimethyl phosphite. No reduction can be observed for 2-methylquinoxaline 1,4-dioxide, whereas in 2-methyl-3-trifluoromethylquinoxaline 1,4-dioxide the NO group in proximity to the electron-withdrawing CF_3 substituent is reduced.[11] If we compare Q_m with some Hammett constants (Table 2), a similar trend is observed for alkyl, carbamoyl and arylazomethine groups in order of increasing electron-withdrawing strength. However, the quinoxaline di-*N*-oxides with carboxyl or alkoxycarbonyl substituents form an exception. The Q_m values of the compounds **26-29** (Table 1; see also Fig. 4) were found to be one order of magnitude lower than expected

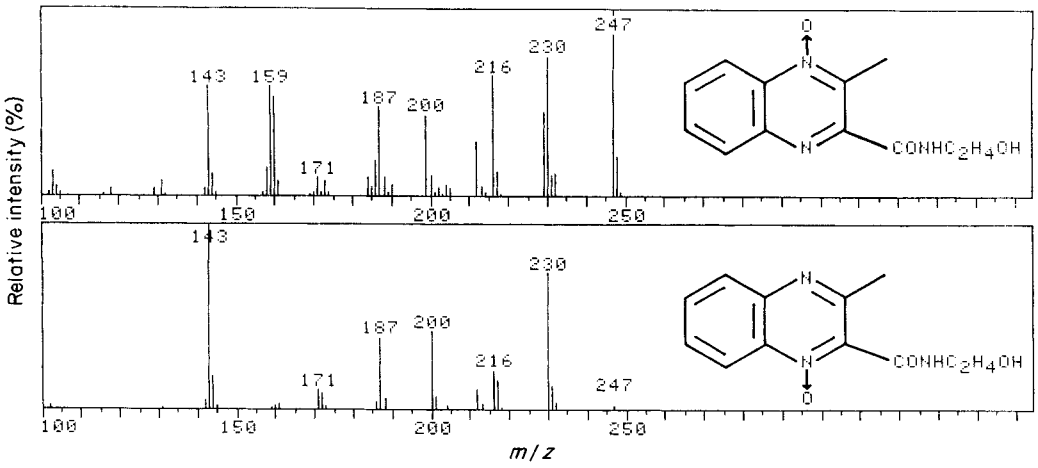

Figure 1. 15 eV mass spectra of the two isomeric 2-methyl-3-*N*-(2-hydroxyethyl)carbamoylquinoxaline mono-*N*-oxides.

(for COOR with averaged values of $\sigma_m = 0.35$ and $\sigma_p = 0.44$: expected $Q_m > 10$; found $Q_m < 1$). Lower-energy pathways for prior degradation of the alkoxycarbonyl group or loss of CO_2 suppress the abundance of $[M-OH]^+$ fragments. Fragments like m/z 176, corresponding to the $[M-CO_2]^{+\cdot}$ fragment in the case of compound **26**, or m/z 203 for the $[M-OR]^+$ fragment in compounds **14** and **28** are characteristic of this behaviour. Moreover, the Q_f values of compounds **26**, **28** and **29** decrease to a level less than 1 which so far has been found only for unsubstituted quinoxaline di-*N*-oxide (**19**).

These results are inconsistent with those of Tatematsu *et al.*[4] who, because of the observed loss of a neutral oxygen atom, generally expected $Q_f < 1$ for quinoxaline di-*N*-oxides. In Fig. 2 two spectra of 2-ethylquinoxaline di-*N*-oxide are compared with each other and additionally there is shown the 2,3-dimethylquinoxaline di-*N*-oxide spectrum (NBS Library spectrum no. 11639 and compounds **21** and **24**). The uncommon loss of oxygen with the resulting intense peak at m/z 174 for the $[M-O]^{+\cdot}$ fragment but no apparent $[M-OH]^+$ seem to be due to the sample introduction via a heated batch inlet system. With the present direct insertion method such a phenomenon was not observed.

Investigation of the NO group effect on degradation of the quinoxaline molecule by linear discriminant analysis

As has been shown, the NO group reacts sensitively to changes in the substitution at the C(2) and C(3) atoms as reflected by the EI induced loss of the OH' radical. On the other hand, *N*-oxidation has a great influence on the electron density distribution in the quinoxaline molecule. Changes in the electron density can be easily observed by ^{13}C-NMR signal shifts[12] (Scheme 1). *N*-Oxidation decreases the electron density at carbon atoms next to the NO group. It is expected that this will significantly influence the mass spectrometric decomposition of the quinoxaline molecule. However, attention should also be paid to another aspect. It is known from photochemistry[13] that irradiation of quinoxaline *N*-oxides yields quinoxalinones (Scheme 2). A similar rearrangement leading to a benzoxazepine has also been

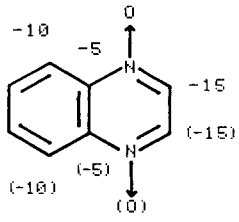

Scheme 1. ^{13}C-NMR shift ($\Delta\delta$) by *N*-oxidation of quinoxalines.

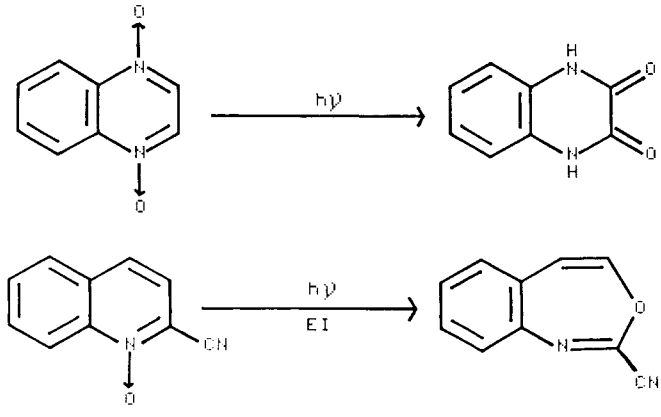

Scheme 2. Rearrangement of heterocyclic *N*-oxides.

Table 2. Values of $Q_m = [M-OH]/[M]$ of substituted quinoxaline di-*N*-oxides and corresponding Hammett constants

R¹	R²	Q_m	Hammett constants[a] σ_m	σ_p	Substituent
Alkyl	H, CH_3	<1	−0.06	−0.14	CH_3
			−0.08	−0.15	C_2H_5
CONR'R''	CH_3	1–10	0.28	0.31	$CONH_2$
R'=H, alkyl R''=H, alkyl			0.35	0.36	$CONHCH_3$
$CH=NC_6H_4R$ R=H, CH_3, Cl, NO_2	H	10–20	0.35	0.42	$CH=NC_6H_5$

[a] cf. Ref. 10.

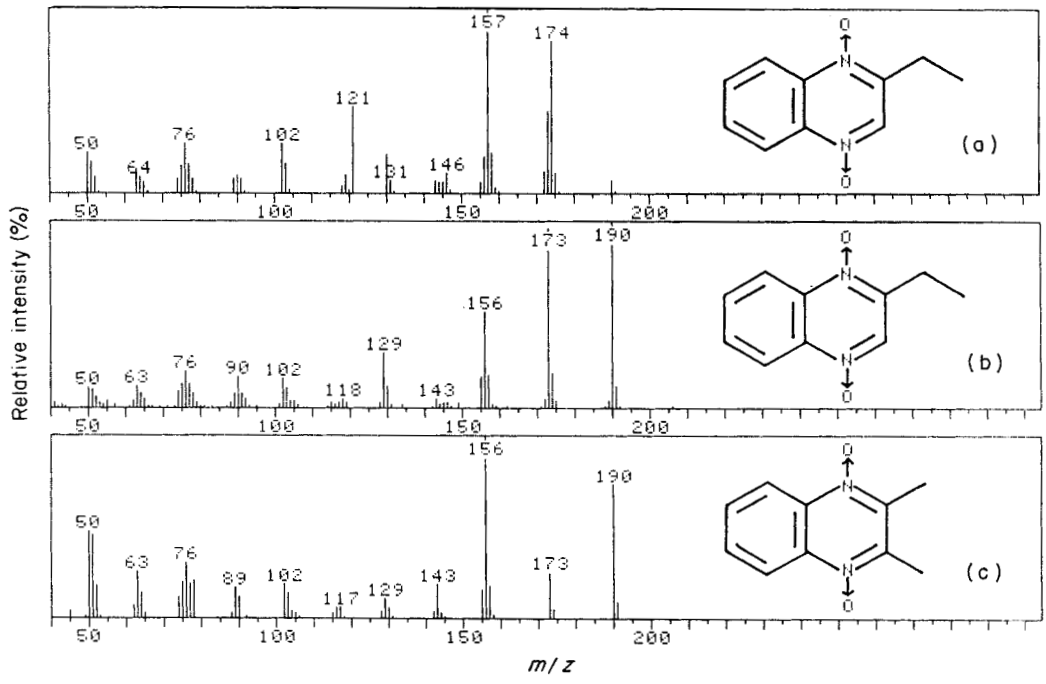

Figure 2. Mass spectra of 2-ethylquinoxaline 1,4-dioxide and 2,3-dimethylquinoxaline 1,4-dioxide from different sources: (a) spectrum no. 11639 from NBS Library; (b) spectrum of compound **21**; and (c) spectrum of compound **24**.

described. Kubo *et al.*[7] found such reactions likewise to be induced by EI. They proved that 2-cyanoquinoline *N*-oxide is rearranged to the 3,1-benzoxazepine, which is characterized by corresponding peaks in the mass spectrum of 2-quinoline *N*-oxide. Accordingly, it was easy to interpret the quinoxaline 1-oxide spectrum as the result of fragmentations starting at two different molecular ions of the same mass which, however, form different primary fragments $[M-O]^{+\cdot}$ and $[M-OH]^{+}$ or $[M-CO]^{+\cdot}$, giving rise to different fragment peak series. As shown in Fig. 3, the spectrum of quinoxaline 1,4-dioxide can be interpreted in a similar manner.

As a result of the substitution at C(2) and C(3) the spectra become rather complicated. In the mass range between m/z 50 and 150 the spectra can be distinguished only by the intensity distribution of the peaks. An answer to the question of to what degree this intensity distribution is characteristic of the number and position of the

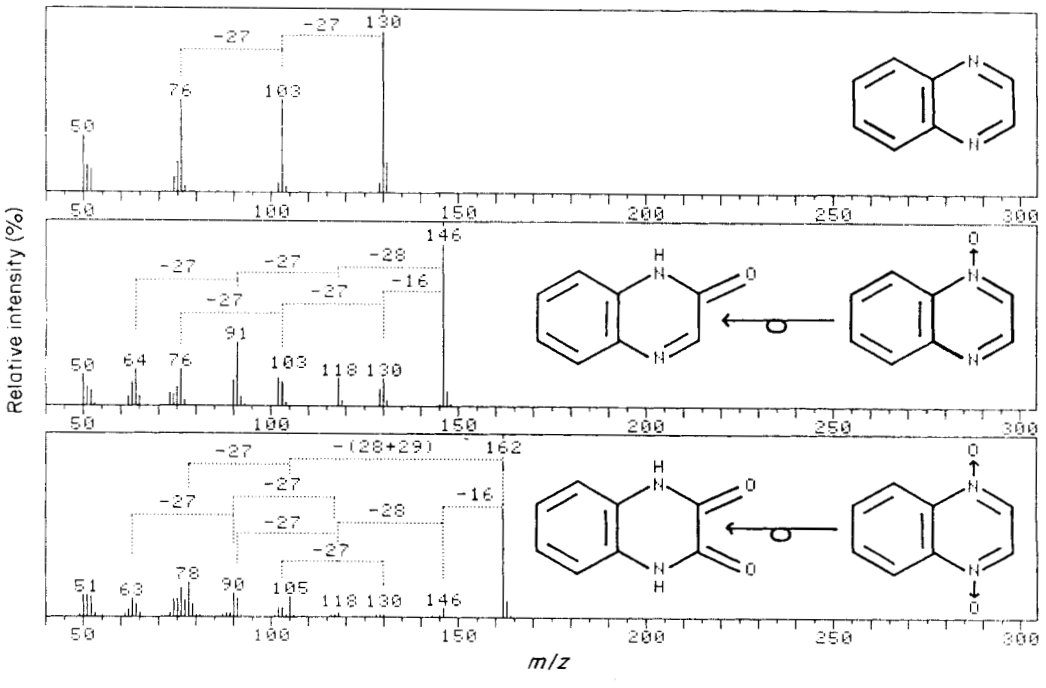

Figure 3. Mass spectra of quinoxaline, quinoxaline 1-oxide and quinoxaline 1,4-dioxide with their fragmentation pathways involving molecular rearrangement.

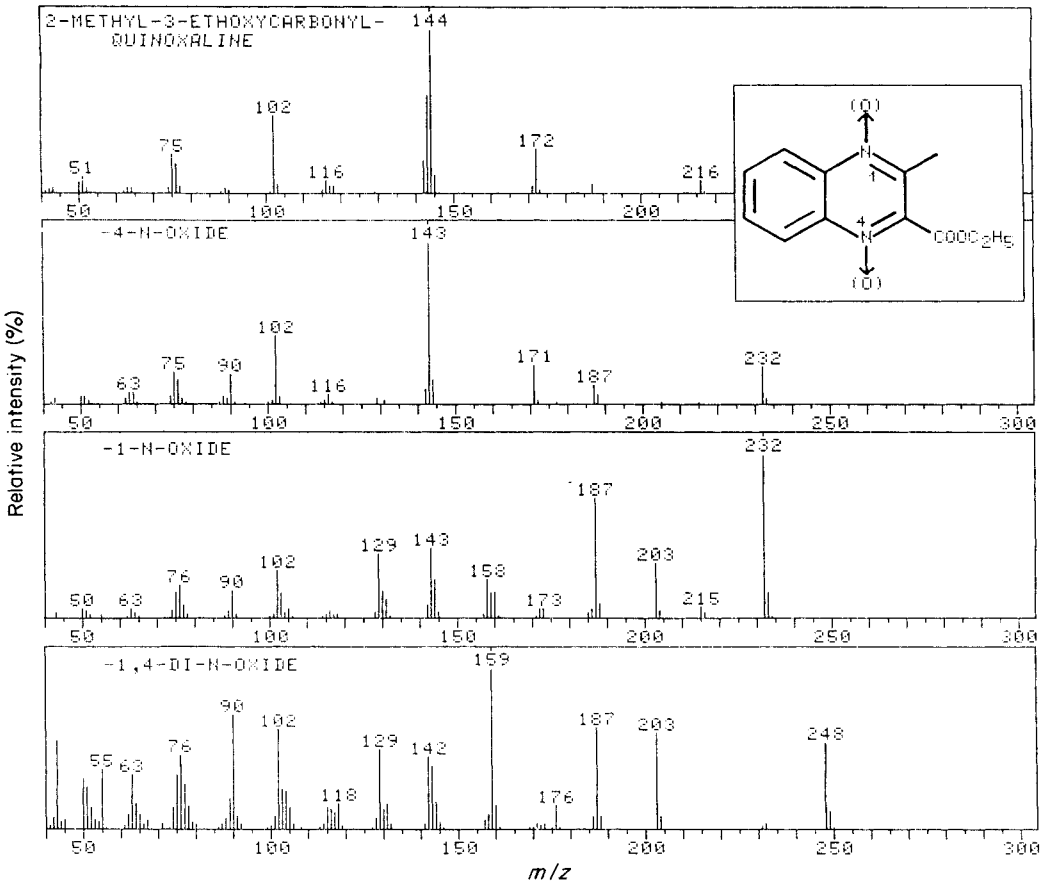

Figure 4. Mass spectra of 2-methyl-3-ethoxycarbonylquinoxaline and the corresponding *N*-oxides.

NO groups can only be given by a comparison of quinoxaline and quinoxaline mono- and di-*N*-oxides all carrying identical substituents (Fig. 4). In order to investigate the influence of the NO groups on the fragmentation of quinoxalines in a detailed manner, the use of statistical methods is essential.

Varmuza[14] gives an extensive review of classification procedures and methods of feature selection. Applications to mass spectrometric problems are also reported. The connection between classificators and mass spectrometric fragmentation reactions was taken into account, but only rarely.[14,16]

For the classification of the quinoxaline spectra with respect to the number of NO groups, a selection of the most relevant features is necessary. As the most discriminating features, the peaks with the highest Fisher quotients[15,16] were selected. These quotients describe the variance of the intensity between the classes in proportion to the variance within the classes for each mass number under consideration:

$$F_i = \sum_{k=1}^{K} (\bar{x}_{ik} - \bar{\bar{x}}_i)^2 \Big/ \sum_{k=1}^{K} V_{ik} \quad (i = 1, 2, \ldots, m)$$

where

K = number of classes
m = number of features
$\bar{x}_{ik}$ = mean value of the patterns of class k in feature i
$\bar{\bar{x}}_i$ = mean value of all patterns in feature i
V_{ik} = variance of the patterns of class k in feature i.

The univariate consideration of the quotients for each feature shows which mass spectrometric fragments are dominated by the different NO group contents and little influenced by the various substituents.

The direction of the NO group influence on peak intensities, however, can only be determined with the help of a multivariate procedure. We decided to study the NO group effect on fragmentation with the help of linear discriminant analysis.[17] The principal ability of discriminant analysis as a method for discriminating between mass spectrometric patterns was shown in a paper by Vink *et al.*[18] A transformation matrix A is determined which maps the original features x_i on to $K-1$ linear independent so-called discriminant features y_j:

$$\begin{bmatrix} y_1 \\ \vdots \\ y_{K-1} \end{bmatrix} = \begin{bmatrix} a_{1,1} & \cdots & a_{1,m} \\ \vdots & & \vdots \\ a_{K-1,1} & \cdots & a_{K-1,m} \end{bmatrix} * \begin{bmatrix} x_1 \\ \vdots \\ x_m \end{bmatrix}$$

$$y_j = \sum_{i=1}^{m} a_{ji} * x_i \quad (j = 1, 2, \ldots, K-1)$$

The rows $\boldsymbol{a}_j = [a_{j1}, \ldots, a_{jm}]$ of this matrix are the discriminant vectors arranged in order of decreasing discriminance. They maximize the quotient

$$\frac{\boldsymbol{a}^{\mathrm{T}} * \boldsymbol{B} * \boldsymbol{a}}{\boldsymbol{a}^{\mathrm{T}} * \mathrm{W} * \boldsymbol{a}}$$

Table 3. Fisher quotients and vector coefficients of the linear discriminant analysis of 63 quinoxaline spectra (discrimination of quinoxalines and their mono- and di-*N*-oxides; 10 from the 20 highest peaks selected)

m/z	Fisher quotient	Vector coefficient	*m/z*	Fisher quotient	Vector coefficient
90	0.73	−0.73	63	0.16	−1.04
76	0.28	1.04	75	0.14	0.40
144	0.25	1.23	129	0.13	−0.74
160	0.25	−0.30	103	0.11	0.79
159	0.20	0.07	143	0.10	−0.56

where B is the covariance matrix of the data between the classes and W the covariance matrix within the classes. Usually they are determined by solution of eigenvalue problems. The vectors $\boldsymbol{a}_j$ define straight lines in the m-dimensional feature space on to which the patterns can be projected with maximal residual discriminance between the classes. In the present case there are three classes (0, 1 and 2 NO groups) and therefore we obtain two discriminant features y_1 and y_2. The orthogonal graphic representation of these two features for all patterns together with the sign and absolute value of the vector coefficients a_{1i} and a_{2i} allow conclusions concerning the connection between the number of NO groups and the peak intensity.

The data base for the first experiment consisted of 63 spectra. Those 20 peaks giving the highest intensity averaged over all spectra were admitted to the statistical feature selection. From these 20 peaks the 10 with the highest Fisher quotients were selected as features for the linear discriminant analysis. The Fisher quotients and the coefficients of the first discriminant vector, which reflects 86% of the discriminance between the three classes (quinoxalines and quinoxaline mono- and di-*N*-oxides), are listed in Table 3. The result of the discriminant analysis is presented graphically in Fig. 5.

Good separation is obtained between the quinoxalines and their *N*-oxides. Discrimination between the mono- and di-*N*-oxides, however, is much more complicated. Extending the data base by incorporating all 20 peaks gives negligible improvement. Table 3 shows that an intense peak at m/z 90 indicates quinoxaline *N*-oxides.

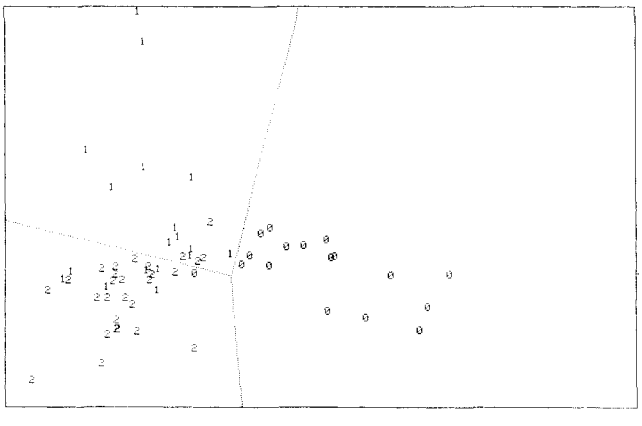

Figure 5. Graphic result of the linear discriminant analysis of 63 quinoxaline spectra (10 from the 20 most intense peaks in the spectra were selected): 0=non-oxidized quinoxalines; 1=mono-*N*-oxides; 2=di-*N*-oxides.

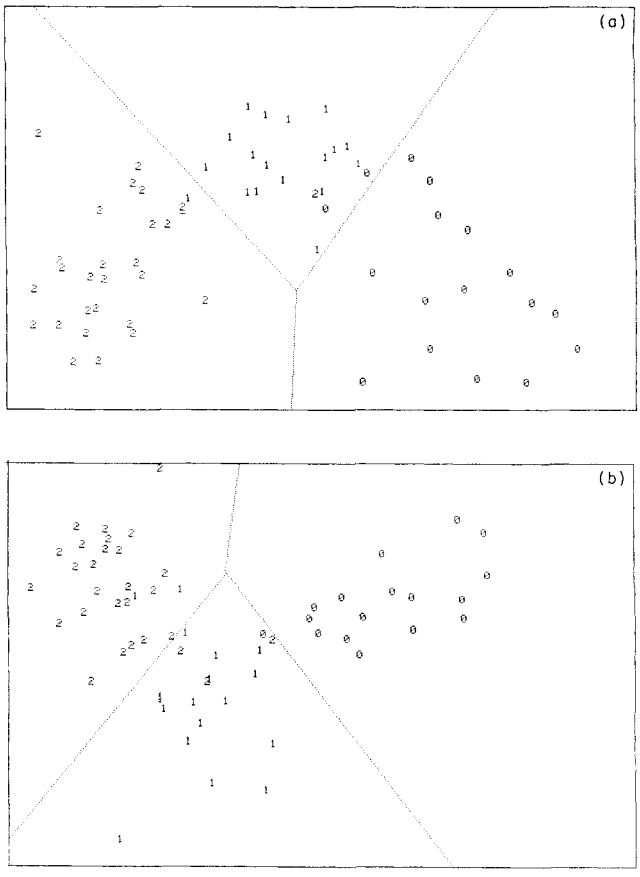

Figure 6. Graphic result of the linear discriminant analysis of 63 quinoxaline spectra. (a) 0%, and (b) 1% relative intensity threshold for selection of peaks: 0=non-oxidized quinoxalines; 1=mono-*N*-oxides; 2=di-*N*-oxides.

Similarly, this holds for all peaks corresponding to a negative coefficient in the first discriminant vector. However, it must be remarked that statements of this kind in the strict sense only hold if the conditions of the linear discriminant analysis are fulfilled (e.g. normal distribution of data). In contrast to the spectra interpretation based on simply considering the relative peak intensities, the discriminant analysis takes into account the frequent possible correlations between the features.

In the second experiment, the 20 peaks with the highest Fisher quotients were selected from all masses as features for the discriminant analysis. With these, an almost complete separation of all classes was achieved (Fig. 6(a)), even if only peaks above 1% relative intensity were admitted to the feature selection (Fig. 6(b)). The peaks m/z 75, 76 and 90 show high Fisher quotients (Table 4). The peak m/z 78 belongs to this group too. According to the signs of the coefficients in the first discriminant vector, intense peaks at m/z 75 and 76 are characteristic of non-oxidized quinoxalines, whereas m/z 78 and 90 appear with higher intensities with quinoxaline *N*-oxides, rather than with the non-oxidized species. The discriminant analysis shows that the molecular rearrangement proven for unsubstituted quinoxalines is also relevant for the species substituted in 2- and 3-positions. Moreover, the discriminant analysis supplies further arguments for the existence of fragmentations involving oxygen rearrangement.

Table 4. Fisher quotients and vector coefficients of the linear discriminant analysis of 63 quinoxaline spectra (discrimination of quinoxalines and their mono- and di-N-oxides; (a) no and (b) 1% relative intensity threshold for selection of peaks as features)

	(a)			(b)	
m/z	Fisher quotient	Vector coefficient	m/z	Fisher quotient	Vector coefficient
76	0.55	0.49	76	0.55	0.50
94	0.53	0.95	90	0.52	−1.45
90	0.51	−1.33	75	0.46	1.00
75	0.46	0.54	128	0.43	0.26
127	0.42	−0.57	114	0.39	−0.43
114	0.41	−0.91	54	0.31	−0.23
128	0.40	−0.50	127	0.30	−1.04
96	0.33	−1.34	66	0.27	0.80
54	0.32	−0.88	144	0.27	0.66
141	0.30	0.04	87	0.27	−0.01
68	0.28	0.09	101	0.26	0.10
144	0.27	0.46	105	0.25	0.34
120	0.26	−0.81	78	0.24	−0.97
105	0.26	0.67	115	0.23	−0.78
101	0.24	0.12	67	0.21	0.04
136	0.23	−0.21	141	0.21	0.36
98	0.23	0.21	56	0.20	−0.32
56	0.23	0.04	159	0.19	0.74
66	0.23	0.78	160	0.19	−0.05
78	0.23	−1.34	94	0.18	0.34

Though of low abundance (<1% relative intensity), the fragments m/z 136 and 120 are interesting as products of a possible 'retro-Beirut' reaction.[12] More frequently, fragments with the mass number m/z 54 appear, which probably originate from transannular fragmentations from quinoxaline N-oxides (Scheme 3).

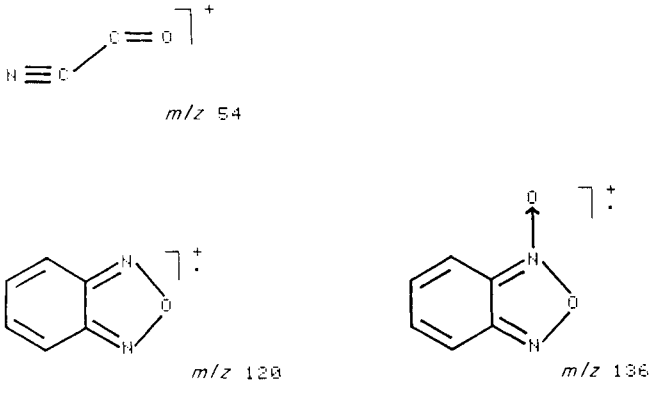

Scheme 3. Ions from possible 'retro-Beirut' and transannular fragmentation found as low-intensity but characteristic peaks by the linear discriminant analysis.

This is an interesting result, but there are some complications in correlating this with the lower-intensity peaks in the spectra. It is not always possible to discover a significant correlation between features relevant for the classification and characteristic fragmentation reactions. Such problems always arise when groups of compounds with a unitary substructure make up the greater part in only one of the classes and when peaks dominated by the structure elements of these groups are selected as features. Thus, the occurrence of the peaks m/z 127 and 128 in the first discriminant analysis (Table 3, Fig. 5) is found to be characteristic of quinoxaline N-oxides but, in contrast, m/z 141 is characteristic of the non-oxidized quinoxalines. In the linked-scan spectra there appears a metastable peak for the elimination of H_2O from the ion m/z 159 giving a fragment m/z 141, suggesting that this peak be classed with quinoxaline N-oxides. Moreover, a detailed study of peak intensities revealed a somewhat higher intensity of these peaks in the spectra of the di-N-oxides. However, the peak intensity of m/z 141 allows us to distinguish between quinoxalines only if they are substituted by a methyl group. Additionally, the interpretation of the results from the discriminant analysis is hampered by inconsistencies of data when library spectra are incorporated. The results given allow us to define the conditions under which the discriminant analysis can be used as an excellent tool for investigating mass spectrometric fragmentations. The fragmentation behaviour of a compound class is reflected the better, the more peaks selected for the classification correspond to fragments containing common structure elements. Thus, defined peaks logically appear in the lower part of the spectra with masses smaller than the mass of the basic molecule. In spite of considerable prior decomposition, the discriminant analysis based on lower mass peaks gives important indications of fragmentation behaviour of the investigated substance class.

In Fig. 7 the graphic result of the discriminant analysis based on m/z 54, 75, 76, 78, 90, 120 and 136 is shown. The clear differentiation between quinoxaline classes with just these seven selected peaks has to be seen as a proof of correct interpretation of the discriminant analysis results. A fragmentation scheme for quinoxalines and their N-oxides based on the present investigations is given in Scheme 4. In addition, metastable decomposition of a number of ions obtained in the linked-scan spectra of compounds **4**, **14**, **15** and **28** is indicated. Elementary composition for most of the fragments shown was determined by high resolution. The fragmentation is dominated by elimination of HCN or CH_3CN and CO. Obviously the fragmentation pathways must be seen as determined by the NO group content, so that the fragments m/z 75, 76, 78 and 90 at the lower end appear useful for classification of quinoxalines. This

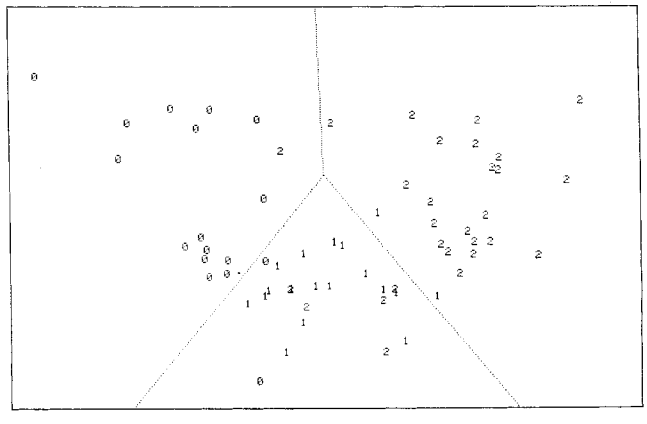

Figure 7. Graphic result of the linear discriminant analysis of 63 quinoxaline spectra (peaks m/z 54, 75, 76, 90, 120 and 136 selected): 0=non-oxidized quinoxalines; 1=mono-N-oxides; 2=di-N-oxides.

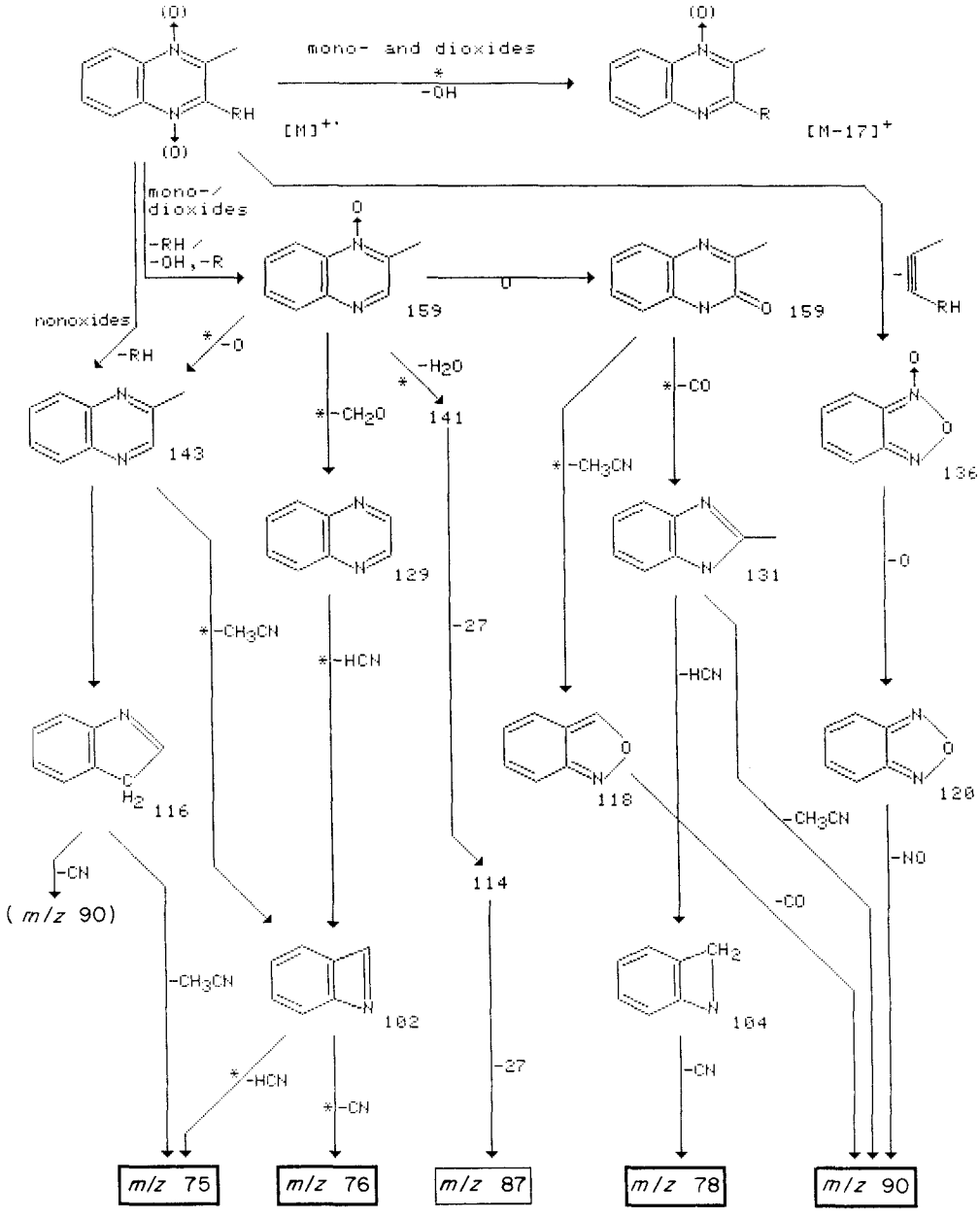

Scheme 4. Main fragmentation pathways of quinoxalines and their *N*-oxides reconstructed from the results of the linear discriminant analysis and metastable peaks from 2-ethoxycarbonyl-3-methylquinoxaline and their *N*-oxides. The fragments *m/z* 78 and 90 are characteristic of quinoxaline *N*-oxides, as is *m/z* 87 but with lower significance. For the non-oxidized quinoxalines, the fragments *m/z* 75 and 76 are found to be characteristic.

result is very important because it proves that rearrangement of quinoxaline *N*-oxides to quinoxalinones prior to mass spectrometric decomposition, as described for unsubstituted quinoxalines, also plays an important part in the large group of the 2- and 3-substituted derivatives investigated.

CONCLUSIONS

In this study of mass spectrometric fragmentation of quinoxalines and their mono- and di-*N*-oxides, we have attempted to answer two questions: how is the loss of oxygen from quinoxaline *N*-oxides influenced by substituents and what results will the presence of NO groups produce under EI conditions? We were able to show that the abundance of the prior OH$^{\cdot}$ loss from *ortho*-substituted quinoxalines increases with the electron-withdrawing strength of the substituent. No difference between mono- and di-*N*-oxides was observed with regard to the dominant loss of OH$^{\cdot}$, in contrast to previously described oxygen elimination with quinoxaline di-*N*-oxides.

In order to answer the second question we disregarded the widely accepted repertoire for investigating mass spectral fragmentations and attempted to obtain an understanding of mass spectrometric behaviour by the use of linear discriminant analysis. This was an exciting experiment. The results of this experiment allow us to say that, in concurrence with decomposition via the loss of OH$^{\cdot}$, the quinoxaline *N*-oxides partially rearrange to

ions with the quinoxalinone structure, so that the mass spectra are formed by several distinct fragment peak series ending at lower mass peaks like the characteristic peaks *m/z* 75, 76, 78 and 90. By means of discriminant analysis, it was possible to determine the NO group influence in a complex form without having to enter into studies of individual cases, thus uncovering hidden correlations between structure and fragmentation of quinoxalines.

EXPERIMENTAL

Preparation of compounds

For the synthesis of previously reported compounds, see Table 1 and references cited therein. Procedures for the preparation of the new compounds are given below.

2-Methyl-3-[*N*-(2-hydroxyethyl)carbamoyl]quinoxaline (5). 2-Ethoxycarbonyl-3-methylquinoxaline (**4**) (10.8 g, 0.05 mol) and ethanolamine (6.1 g, 0.1 mol) in 60 cm^3 methanol were stirred at room temperature for 8 h. The precipitated **5** was filtered off, washed with a small amount of methanol and dried: yield, 3.5 g (30%); m.p., 118–120 °C (after extraction with *n*-hexane); analysis,

$C_{12}H_{13}N_3O_2$	calc.	C, 62.32;	H, 5.67;	N, 18.17
(231.26)	found	61.95	5.72	17.93

2-Ethoxycarbonyl-3-methylquinoxaline 1-oxide (14) and 3-ethoxycarbonyl-2-methylquinoxaline 1-oxide (15). These were prepared according to the general procedure of Dirlam and McFarland[11] by reduction of the 1,4-dioxide **28**. **14**: m.p., 86–88 °C; NMR (DMSO-d_6), δ 1.39 (3, t, CH_3), 2.60 (3, s, CH_3), 4.52 (2, q, CH_2), 7.70 (2, m, H-6, H-7), 7.95 (1, m, H-5), 8.45 (1, m, H-8); analysis,

$C_{12}H_{12}N_2O_3$	calc.	C, 62.06;	H, 5.21;	N, 12.06
(232.24)	found	61.87	5.01	11.93

15: m.p., 92–93 °C; NMR (DMSO-d_6), δ 1.37 (3, t, CH_3), 2.56 (3, s, CH_3), 4.42 (2, q, CH_2), 7.82 (2, m, H-6, H-7), 8.07 (1, m, H-8), 8.34 (1, m, H-5).

2-Methyl-3-[*N*-(2-hydroxyethyl)carbamoyl]quinoxaline 4-oxide (16). **13** (10.9 g, 0.05 mol) and ethanolamine (6.1 g, 0.1 mol) in 100 cm^3 methanol were stirred at 50 °C for 4 h. After standing overnight the precipitated **16** was filtered off, washed with a small amount of methanol and dried: yield, 6.3 g (51%); m.p., 166–168 °C (from methanol); analysis,

$C_{12}H_{13}N_3O_3$	calc.	C, 58.29;	H, 5.30;	N, 17.00
(247.26)	found	57.93	5.12	17.30

2-Methyl-3-[*N*-(2-hydroxyethyl)carbamoyl]quinoxaline 1-oxide (17). **15** (11.6 g, 0.05 mol) and ethanolamine (6.1 g, 0.1 mol) in 100 cm^3 methanol were stirred at room temperature for 2 h. The precipitated **17** was filtered off and dried: yield, 8.9 g (72%); m.p., 139–140 °C; analysis,

$C_{12}H_{13}N_3O_3$	calc.	C, 58.29;	N, 5.30;	N, 17.00
(247.26)	found	57.95	5.17	17.21

2-Methyl-3-[*N*,*N*-bis(2-hydroxyethyl)carbamoyl]quinoxaline 1,4-dioxide (35). **28** (12.4 g, 0.05 mol) and diethanolamine (10.5 g, 0.1 mol) in 60 cm^3 methanol were stirred for 8 h at 60 °C. After standing overnight at room temperature, **35** was filtered off, washed with a little methanol and dried: yield, 7.90 g (51%); m.p., 198–202 °C; analysis,

$C_{14}H_{17}N_3O_5$	calc.	C, 54.72;	H, 5.58;	N, 13.67
(307.31)	found	54.65	5.67	13.83

2-Bromomethyl-3-[*N*-(2-hydroxyethyl)carbamoyl]quinoxaline 1,4-oxide (36). A suspension of **34** (26.3 g, 0.1 mol) in 250 cm^3 methylene chloride and 300 ml DMF was heated under reflux. Bromine (19.2 g, 0.12 mol) was then added dropwise while stirring and the reaction mixture maintained for 5 h at this temperature. After cooling the solid was filtered off, washed with methanol and dried: yield, 27.4 g (80%); m.p., 198–201 °C (from DMF/ethanol); analysis,

$C_{12}H_{12}BrN_3O_4$	calc.	C, 42.12;	H, 3.54;	N, 12.28
(342.17)	found	42.10	3.42	11.98

2-Acetoxymethyl-3-[*N*-(2-hydroxyethyl)carbamoyl]quinoxaline 1,4-dioxide (37). **36** (34.2 g, 0.1 mol) was suspended in 100 cm^3 ethanol while stirring and heated under reflux. A solution of sodium acetate (16 g) in 25 cm^3 water was added dropwise. After the addition was complete, the mixture was refluxed for 4 h and cooled to room temperature, and the solid filtered off, washed with a small amount of ethanol and dried: yield, 23.4 g (73%); m.p., 170–172 °C (from ethanol); analysis

$C_{14}H_{15}N_3O_6$	calc.	C, 52.34;	H, 4.71;	N, 13.08
(321.29)	found	52.36	4.67	12.86

2-(Aryliminomethyl)quinoxalines (9, 10). General procedure: a mixture of 2-formylquinoxaline (0.01 mol) and the requisite nitroaniline (0.01 mol) in 30 cm^3 ethanol was heated under reflux for 5 min and cooled, and the

Table 5. Physical and analytical data for 2-(aryliminomethyl)-quinoxalines and 2-(aryl(alkyl)iminomethyl)quinoxaline 1,4-di-*N*-oxides

Compound	Mol. wt	Yield (%)	M.p. (°C)	Elemental analysis (calc./found)(%) C	H	N
9	278.28	83	209–210	64.74	3.62	20.13
				64.57	3.64	20.27
10	278.28	68	218–223	64.74	3.62	20.13
				64.79	3.59	20.09
38	245.28	60	110–112	63.66	6.16	17.13
				63.47	6.25	17.05
39	271.33	53	134–138	66.40	6.32	15.49
				66.54	6.30	15.34
40	265.27	84	194–198	67.92	4.18	15.84
				68.17	4.35	15.63
41	279.31	83	195–201	68.80	4.69	15.05
				69.15	4.65	14.96
42	299.73	78	212–218	60.11	3.36	14.02
				59.97	3.33	13.87
43	310.28	63	218–220	58.06	3.25	18.06
				57.94	3.34	17.87

solid filtered off, washed with water and dried (see Table 5).

2-(Aryl(alkyl)iminomethyl)quinoxaline 1,4-dioxides (38–43). General procedure: 2-formylquinoxaline 1,4-dioxide (0.01 mol) was suspended in 20 cm^3 methylene chloride and cooled to 0 °C. A solution of the requisite amine in 15 cm^3 methylene chloride was then added dropwise *while stirring*, and the precipitated solid filtered off and dried (see Table 5).

Mass spectrometry

Low-resolution mass spectra were run on a HP 5985 B GC/MS system using a modified direct insertion probe which allows heating rates up to 200 °C min^{-1} for rapid evaporation. EI parameters: electron energy, 70 eV; emission current, 300 μA; source temperature, 200 °C. *B/E* linked scans for metastable peak detection were carried out on a Finnigan MAT 212. Computer programs for the linear discriminant analysis were written in FORTRAN IV for on-line data handling with the HP 5985 B system and its HP 1000 computer having 32 K memory.

The following spectra from the NBS Library were added to our own data base for linear discriminant analysis: spectrum nos. 3666, 5388, 5665, 7247, 7741, 7742, 9327, 9511, 9512, 9513, 9928, 11202, 11428, 11639, 11640, 13364, 13188 and 20224.

REFERENCES

1. A. R. Katrizky (Ed.), *Comprehensive Heterocyclic Chemistry*, Vol. 1, p. 220. Pergamon, Oxford (1984).
2. G. K. Figdor and D. C. Hobbs, *Can. J. Chem.* **58**, 1957 (1980).
3. W. Suter, A. Rosselet and F. Knüsel, *Antimicrobial Agents and Chemotherapy* **13**, 770 (1978).
4. A. Tatematsu, H. Yoshizumi, E. Hayashi and H. Nakata, *Tetrahedron Lett.* 2985 (1967).
5. D. A. Lightner, R. Nicoletti, G. B. Quistad and E. Irwin, *Org. Mass Spectrom.* **4**, 571 (1970).
6. V. Kovaćik, M. Fedorenko and I. Jezo, *Org. Mass Spectrom.* **7**, 449 (1973).
7. A. Kubo, S. Sakai, S. Yamada, I. Yokoe, C. Kaneko, A. Tatematsu, H. Yoshizumi, E. Hayashi and N. Nakata, *Chem. Pharm. Bull.* **15**, 1079 (1967).
8. R. Grigg and B. G. Odell, *J. Chem. Soc. B* 218 (1966).
9. N. Bild and M. Hesse, *Helv. Chim. Acta* **50**, 1885 (1967).
10. N. B. Chapmann and J. Shorter (Eds), *Correlation Analysis in Chemistry*, pp. 439–541. Plenum, New York (1978).
11. J. P. Dirlam and J. W. McFarland, *J. Org. Chem.* **42**, 1360 (1977).
12. A. F. Kluge, M. L. Maddox and G. S. Lewis, *J. Org. Chem.* **45**, 1909 (1980).
13. O. L. Chapman (Ed.), *Organic Photochemistry*, Vol. 2, pp. 117–62. Marcel Dekker, New York (1969).
14. K. Varmuza, *Pattern Recognition in Chemistry*. Springer, Berlin (1980).
15. B. R. Kowalski (Ed.), *Chemometrics, Theory and Application*, p. 43. American Chemical Society, Washington, DC (1977).
16. E. Ziegler (Ed.), Computer in der Chemie. Springer, Berlin (1984).
17. H. Ahrens and J. Läuter, *Mehrdimensionale Varianzanalyse*. Akademie-Verlag, Berlin (1981).
18. J. Vink, W. Heerma, J. P. Kamerling and J. F. G. Vliegenthart, *Org. Mass Spectrom.* **9**, 536 (1974).
19. A. Weissberger and E. C. Taylor (Eds), *The Chemistry of Heterocyclic Compounds*, Vol. 35. Wiley, New York (1979), and references therein.
20. A. S. Elina and L. G. Tsyrul'nikova, *Zh. Obshch. Khim.* **34**, 2077 (1964); *Chem. Abs.* **61**, 8308 e (1964).
21. F. Wegland, H.-J. Bestman and H. Fritsche, *Chem. Ber.* **93**, 2340 (1960).
22. A. Kjaer, *Acta Chem. Scand.* **2**, 455 (1948).
23. C. L. Leese and N. N. Rydon, *J. Chem. Soc.* 303 (1955).
24. S. J. Benkovic, P. A. Benkovic and R. Chrzanowski, *J. Am. Chem. Soc.* **92**, 523 (1970).
25. J. K. Landquist and J. A. Silk, *J. Chem. Soc.* 2052 (1956).
26. M. J. Haddadin, H. N. Alkaysi and S. E. Saheb, *Tetrahedron* **26**, 1115 (1970).
27. M. J. Abu El-Haj, T. H. Cronin and K. Richardson, DE-OS 2111710 (1971); *Chem. Abs.* **76**, 3900 y (1972).
28. K. Ley and F. Seng, *Synthesis* 415 (1975).
29. K. Ley, U. Eholzer, K.-G. Metzger and D. Fritsche, DE-OS 1670935 (1967); *Chem. Abs.* **71**, 91528 h (1969).
30. Sukale, H.-J. Niclas, H.-J. Richter and M. Bohle, DD 234866 (1985).